

An Upper Limit on the Temporal Variations of the Solar Interior Stratification

A. Eff-Darwich^{1,2,5} and S.G. Korzennik¹

S.J. Jiménez-Reyes^{2,3}

F. Pérez Hernández^{2,4}

¹*Harvard-Smithsonian Center for Astrophysics, 60 Garden St., Cambridge, MA, 02138 MS16*

²*Instituto de Astrofísica de Canarias, C/ Vía Láctea s/n, Tenerife, 38205, Spain*

³*High Altitude Observatory, National Center for Atmospheric Research, 1850 Table Mesa Dr. Boulder, Colorado 80307*

⁴*Departamento de Astrofísica, Universidad de La Laguna, Tenerife, Spain*

ABSTRACT

We have analyzed changes in the acoustic oscillation eigenfrequencies measured over the past 7 years by the GONG, MDI and LOWL instruments. The observations span the period from 1994 to 2001 that corresponds to half a solar cycle, from minimum to maximum solar activity.

These data were inverted to look for a signature of the activity cycle on the solar stratification. A one-dimensional structure inversion was carried out to map the temporal variation of the radial distribution of the sound speed at the boundary between the radiative and convective zones. Such variation could indicate the presence of a toroidal magnetic field anchored in this region.

We found no systematic variation with time of the stratification at the base of the convection zone. However we can set an upper limit to any fractional change of the sound speed at the level of 3×10^{-5} .

Subject headings: Sun: helioseismology, interior, magnetic fields

1. Introduction

Changes in the frequency of the solar p -mode oscillations have now been observed for more than a decade. Such changes affect both the central frequencies, ν_{nl} , and the frequency splittings, $\Delta\nu_{nlm}$ of low degree (Jiménez-Reyes *et al.* 2001), intermediate degree (Howe *et al.* 1999; Dziembowski *et al.* 2000) and very high degree modes (Rajaguru *et al.* 2001). A number of mechanisms have been proposed to explain these variations on frequency. Libbrecht & Woodard (1990) have argued, on the basis of observations of intermedi-

ate degree modes, that the source of the perturbations must lie near the solar surface. Gough & Thompson (1988) and Paternó (1990) concluded that magnetic fields located near the base of the convection zone, with strengths significantly lower than 10^6 G have no observable effect on p -mode frequencies. The stability analysis for magnetic fields by Moreno-Insertis *et al.* (1992) has shown that fields with strengths significantly larger than 10^5 G cannot be stored in this region.

The p -mode frequency variations track rather well the changes of the activity strength of the solar cycle with time. It is thus plausible that these frequency shifts are due to variations of the mean magnetic field near the photosphere (Gough

⁵present address: Department of Soil Sciences and Geology, University of La Laguna, Tenerife, 38205, Spain

& Thompson 1988; Goldreich *et al.* 1991). The influence of thin magnetic fibrils on the frequency shifts has been investigated by Bogdan & Zweibel (1985). Another possible cause for these frequency shifts is the presence of sunspots during solar activity (Braun *et al.* 1992). The dominant effect of sunspots on the propagation of acoustic waves is believed to be the dissipation of the acoustic energy and therefore, should decrease their amplitudes and lifetimes (Hindman & Brown 1998; Rajaguru *et al.* 2001), while it has been observed that frequencies increase with increased magnetic activity.

In the work presented here, we explore a mechanism first suggested by Kuhn (1988), in which the sound speed perturbation associated to the observed changes of the photospheric latitudinal temperature distribution might be responsible for the frequency shifts seen during the solar cycle. Changes in the temperature distribution are themselves due to the heat transport through the convection zone induced by the solar dynamo.

Let us suppose that there is a magnetic field anchored below the base of the convection zone. To maintain pressure equilibrium, the gas pressure and thus the density inside the magnetized region must be lower than in its surroundings. The magnetized fluid will thus experience a larger radiative heating and therefore the temperature at the top of the magnetized region will increase. This will also induce a change in the temperature gradient that could be large enough to make the region above the magnetic field convectively unstable. In such a scenario, the base of the convection zone would locally drop, allowing the magnetized fluid to ascend by convective upflows, transporting excess entropy to the photosphere (Kuhn & Stein 1996).

Numerical experiments by Kuhn & Stein (1996) have shown that entropy perturbations in the deep convection zone can produce strongly peaked temperature changes in regions below $\tau = 1$ that have a substantial acoustic signature (where τ is the optical depth). They have also shown that the thermal perturbations that account for the solar acoustic variability are consistent with the observed solar irradiance and luminosity changes that occur during the 11 year solar cycle.

Luminosity changes, even if no larger than 0.1%, must come from the release of energy

stored somewhere in the solar interior and must be accompanied by a change in the solar radius. The ratio between relative luminosity and radius changes, hereafter W , can help estimate the location of the region where this energy is stored (Gough 2000, and references therein). Theoretical calculations indicate that W increases when increasing the depth of the source of the variations in luminosity. For instance $W \approx 2 \cdot 10^{-4}$ if the source is located in the outer layers of the convection zone, while $W \approx 0.5$ if the source is located in the solar core. Unfortunately there is a large scatter in the observed values of W . Indeed, recent measurements of W range from 0.021 as estimated by Dziembowski *et al.* (2001) and Antia *et al.* (2000a) to an upper limit of 0.08 derived by Emilio *et al.* (2000).

Kuhn (2000) estimated that a 0.1% luminosity perturbation integrated over a solar cycle corresponds to about 10^{39} erg. If this energy originates in the tachocline and if the tachocline thickness is $0.05 R_{\odot}$, the associated relative variation in sound speed at that depth would be on the order of $\delta c/c \approx 10^{-5}$ or 10^{-6} . Fractional changes in sound speed as small as 10^{-4} are easily accessible by helioseismic inversion techniques. Some attempts to find solar-cycle variations of the sound speed asphericity and the latitude-averaged sound speed have been carried out using MDI and/or GONG data (Dziembowski *et al.* 2001; Howe *et al.* 1999; Antia *et al.* 2000b; Antia *et al.* 2001; Basu & Antia 2001). However, none of them found any systematic variation of the solar structure at the base of the convection zone that could be associated with the presence of a local toroidal magnetic field.

We have extended the previous analysis to the latest data available, including LOWL data. Only common modes to all data sets were used, in an attempt to obtain comparable and significant results to all instruments. This way, we can give a robust upper limit on the temporal variations of the solar internal stratification during the period 1994-2001.

2. Inversion Technique

The inversion for solar structure, in particular sound speed c and density ρ , are commonly based on the linearization of the equations of stellar oscillations around a reference model (Gough & Koso-

vichev 1988; Dziembowski *et al.* 1990; Gough & Kosovichev 1990). The differences of the structural profile between the actual sun and a model are linearly related to differences between the observed frequencies and those calculated using that model. This relation is obtained using a variational formulation for the frequencies of adiabatic oscillations. A general relation for frequency differences is given by

$$\frac{\delta\nu_{nl}}{\nu_{nl}} = \int_0^{R_\odot} \left[K_{c,\rho}^{nl}(r) \frac{\delta c}{c}(r) + K_{\rho,c}^{nl}(r) \frac{\delta\rho}{\rho}(r) \right] (\mathbf{d}\mathbf{r}) + \mathcal{E}_{nl}^{-1} F(\nu) + \epsilon_{nl}$$

where $\delta\nu_{nl}$ are the frequency differences between the actual sun and the model for the mode with radial order n and degree l , and ϵ_{nl} the corresponding relative error. The sensitivity functions, or kernels, $K_{c,\rho}^{nl}(r)$ and $K_{\rho,c}^{nl}(r)$ are known functions, that relate the changes in frequency to the changes in the model. The functions $\delta c/c$ and $\delta\rho/\rho$ are the unknown parameters to be inverted, *i.e.*: the relative difference in the sound speed and the density respectively, and R_\odot is the solar radius. The term $\mathcal{E}_{nl}^{-1} F(\nu_{nl})$ in Eq. 1 is introduced to take into account the so-called surface uncertainties; these include the dynamical effects of convection on the oscillation equations, as well as non-adiabatic processes in the near-surface layers (see Dziembowski *et al.* 1990, and references therein).

Following standard procedures, we represent $F(\nu_{nl})$ as a Legendre polynomial expansion. \mathcal{E}_{nl} is the inertia of the mode, normalized by the inertia that a radial mode of the same frequency would have (for more details, see Gough & Thompson 1991).

If we take $\delta\nu_{nl}$ as the differences in the observed frequencies at two different epochs, rather than the differences in frequency between the actual sun and the model, $\delta c/c$ and $\delta\rho/\rho$ represent the variation with time of the sun's internal structure, as long as our underlying theoretical model is very close to the actual sun.

The inverse problem defined by Eq. 1 is well known to be an ill-posed problem (Thompson 1995), whose solution is not unique. It can be solved using inversion methodologies that can be classified in two different techniques: the regularized least-squares methods (RLS, see Craig &

Brown 1986) and the optimal localized average methods (OLA, Backus & Gilbert 1968). Both methods compute an estimate of the solution at a target location from a linear combinations of the observables, given a mesh of target locations. We have developed a variant of the RLS technique, that we call the optimal mesh distribution (OMD), that optimizes the mesh of target locations to avoid undesired high-frequency oscillations of the solution. This optimization is achieved by computing *a priori* the spatial resolution of the solution from the set of available observables and their uncertainties (Eff-Darwich & Pérez-Hernández 1997). The smoothing function is itself defined also from the spatial resolution analysis and it is weighted differently for each radial point. This method ensures that the smoothing constraint is properly applied over the optimal mesh.

3. Observational Data

The observational data consist of mode frequencies computed from time series spanning different epochs and observed with different instruments. Namely, 57 sets based on 108-day-long time series derived from the GONG instruments (Leibacher *et al.* 1996) and spanning May 1995 to February 2001; 27 sets based on 72-day-long time series derived from the MDI instrument (Schou 1999) and spanning May 1996 to November 2001; and 6 sets based on 1-year-long time series derived from the LOWL instrument (Jiménez-Reyes 2000; Tomczyk *et al.* 1995) and spanning 1994 to 1999.

In order to use consistent data sets, only the modes common to all the sets for a given instrument were taken into account. As a consequence, the low degree modes ($l < 13$) present in some GONG data sets had to be rejected. Also this selection reduces the number of MDI and LOWL modes by 30% and 4% respectively.

The MDI and LOWL sets were further reduced to only include the modes common to both instruments. This was not done with the GONG data set due to the small amount of common modes present. Finally, and again for consistency, we deliberately restricted range of degrees we included to correspond to the highest degree available in the LOWL data set (*i.e.*, $l \leq 100$).

For each instrument and for each mode we com-

puted the temporal frequency average. We subsequently subtracted the respective averaged frequencies from each set, leaving us with frequency changes with respect to this temporal average as a function of epoch. For the GONG and MDI sets, we also computed averages corresponding to 1-year-long epochs. Such averaging reduced the scatter of the data while producing data sets comparable to the LOWL sets.

4. Results

Figure 1 shows the relative change of the sound speed as a function of radius inferred from 1-year-long MDI, GONG and LOWL sets. These profiles show no significant changes at the level of a few times 10^{-5} . The precision and resolution of the inversion is good enough to detect small variations of the stratification at the base of the convection zone. This is demonstrated in Fig. 2, where we show the sound speed profiles inferred from the 1996 averaged MDI, GONG and LOWL data sets as well as sound speed profiles obtained by inverting the same mode sets, but after injecting frequency changes that result from a perturbation in the sound speed (as small as 3×10^{-6} and 3×10^{-5}) between 0.68 and $0.70 R_{\odot}$. This figure indicates that a perturbation of the sound speed at the base of the convection zone on the order of, or slightly smaller than 5×10^{-5} , can be detected with the current precision resulting from 1-year-long time-series. Perturbations on the order of 10^{-6} fall in the noise level of our inversions.

In an attempt to find temporal variations of the solar stratification at the base of the convection zone, we computed the mean value of $\delta c/c$ in the radial interval $0.69 \leq r/R_{\odot} \leq 0.72$. This interval contains not only the base of the convection zone, $r \approx 0.7133 R_{\odot}$ (Basu & Antia 2001), but also the tachocline, $r \approx 0.691 R_{\odot}$ (Corbard *et al.* 1999), both closely related to the toroidal magnetic field responsible of the solar cycle. The resulting values are shown as a function of time in Fig. 3, for the inversions based on 1-year-long sets for all three instruments (GONG, MDI and LOWL), as well as on the GONG 108-day-long and MDI 72-day-long sets.

Inversion profiles inferred from any linear inversion technique always correspond to the convolution of the underlying solution by the resolution

kernel (Thompson 1995). Therefore, even if the mode set used in a sequence of inversions remains identical, the resolution kernels will, at some level, change with time since the uncertainties change with time. Such variation could produce an *apparent* temporal behavior of the inferred profiles that does not correspond to a *real* variation of the underlying *true* solution. To quantify this effect, we computed the averaging kernels at $r = 0.69 R_{\odot}$ for all the inversions based on 1-year-long data sets. These were convolved with an artificial sound speed perturbation of the form:

$$\frac{\delta c}{c} = \begin{cases} 3 \times 10^{-5} & \text{for } 0.67 \leq r/R_{\odot} \leq 0.71 \\ 5 \times 10^{-5} & \text{for } 0.91 \leq r/R_{\odot} \leq 0.93 \\ 0 & \text{otherwise} \end{cases} \quad (2)$$

where the sound speed perturbation centered at $0.92 R_{\odot}$ attempts to reproduce the results found by Dziembowski *et al.* (2000); Antia *et al.* (2001), while a second perturbation at the base of the convection zone is also introduced. The convolutions $q_{r_o}(t)$ are then calculated in the following way:

$$q_{r_o}(t) = \int K(r, r_o, t) \frac{\delta c(r)}{c(r)} dr \quad (3)$$

The resulting values of $q_{r_o}(t)$, at $r_o = 0.69 R_{\odot}$, relative to the average q_{av} of all the convolutions calculated for every instrument, are shown in Fig. 4. This figure demonstrates that for the data from all three instruments the effect of the changes in the observed uncertainties on the inverted profiles is negligible, corresponding to levels well below 10^{-7} .

The averaging kernel corresponding to the solution at $r = 0.69 R_{\odot}$ obtained from the 1997 MDI data set is shown in the right panel of Fig. 5. This is well located and indicates that our radial resolution corresponds to $0.04 R_{\odot}$. We should also point out that the averaging kernels have an important negative non-local contribution near the surface, a feature that affect at some level the solution at the base of the convection zone. The effect of this non-local component of the averaging kernels was quantified, in the case of MDI and GONG data, by performing inversions with data sets expanded to higher degrees, *i.e.*, up to $l = 150$. The averaging kernel at $r = 0.69 R_{\odot}$ obtained from the MDI 1997 data shows a substantial reduction of the negative component located at $r \approx 0.90 R_{\odot}$ when including

higher degree modes. But the temporal behavior of the stratification at the base of the convection zone do not significantly differ when the MDI data sets are expanded from $l \leq 100$ to $l \leq 150$, as illustrated in the left panel of Fig. 5.

Therefore, by including the data from all three instruments, and after assessing the effects of temporal changes of the resolution of the solutions, we can safely conclude that there is not significant systematic variations of the stratification at the base of the convection zone at the level of 3×10^{-5} , and that this upper limit is constrained by the scatter present in the data.

Vorontsov (2000) analyzed MDI data spanning from 1996 to 2000 and found systematic variations of the radial solar stratification with time, expressed as relative changes of radius of 2×10^{-5} . Our results obtained with MDI data are in good agreement with those found by Vorontsov (2000), in the sense that there is a systematic variation in the relative sound speed difference that is well correlated to the magnetic activity in the Sun. The maximum in solar activity corresponds to the maximum variation in sound speed. Since these results are not seen when analyzing LOWL and GONG data they should still be taken with some degree of scepticism.

5. Acknowledgments

The Solar Oscillations Investigation - Michelson Doppler Imager project on SOHO is supported by NASA grant NAS5-3077 at Stanford University. SOHO is a project of international cooperation between ESA and NASA.

The GONG project is funded by the National Science Foundation through the National Solar Observatory, a division of the National Optical Astronomy Observatories, which is operated under a cooperative agreement between the Association of Universities for Research in Astronomy and the NSF.

The LOWL instrument has been operated by the High Altitude Observatory of the National Center for Atmospheric Research which is supported by the National Science Foundation.

This work was partially supported by NASA - Stanford contract PR-6333 and by NSF grant AST-95-2177.

REFERENCES

- Antia, H. M., Basu, S., Pintar, J., & Pohl, B. *Sol. Phys.*, 192, 459, 2000a.
- Antia, H. M., Chitre, S. M., & Thompson, M. J. *A&A*, 360, 335, 2000b.
- Antia, H. M., Basu, S., Hill, F., Howe, R., Komm, R. W., & Schou, J. *MNRAS*, 327, 1029, 2001
- Backus, G., Gilbert, F., 1968, *Geophys. J. R. Astron. Soc.* 16, 169
- Basu, S. & Antia, H. M. *MNRAS*, 324, 498, 2001
- Bogdan, T.J., Zweibel, E.G. *ApJ*, 298, 867, 1985.
- Braun, D.C. *et al.* *ApJ*, 391, L113, 1992.
- Corbard, T., Blanc-Féraud, L., Berthomieu, G., & Provost, J. *A&A*, 344, 696, 1999.
- Craig, I.J.D, Brown, J.C. *in Inverse Problems in Astronomy: A Guide to Inversion Strategies for Remotely Sensed Data (Bristol: A. Hilger)*, 1986.
- Dziembowski, W., Pamyatnykh, A.A., Sienkiewicz, R. *MNRAS*, 244, 542, 1990.
- Dziembowski, W. A., Goode, P. R., Kosovichev, A. G., & Schou, J. *ApJ*, 537, 1026, 2000.
- Dziembowski, W. A., Goode, P. R., & Schou, J. *ApJ*, 553, 897, 2001.
- Eff-Darwich, A. Pérez-Hernández, F. *A&ASS*, 125, 1, 1997.
- Emilio, M., Kuhn, J. R., Bush, R. I., & Scherrer, P. 2000, *ApJ*, 543, 1007
- Goldreich, P. Murray, N. Willette, G., Kumar, P. *ApJ*, 370, 752, 1991.
- Gough, D.O. *Nature*, 272, 1282, 2000.
- Gough, D.O., Kosovichev, A.G. *in Berthomieu and Cribier eds., Inside the Sun, Dordrecht, Kluwer*, p. 327, 1990.
- Gough, D.O., Kosovichev, A.G. *in Seismology of the Sun and Sun-like stars (ESA SP-286)*, p. 195, 1988.

- Gough, D.O., Thompson, M.J. in *A.N. Cox, W.C. Livingston, M.S. Matthews eds., Solar Interior and Atmosphere*, p. 519, 1991.
- Gough, D.O., Thompson. M.J. in *Christensen-Dalsgaard and Frandsen eds., Advances in Helio- and Asteroseismology, Reidel, Dordrecht, IAU Symp.*, p. 123, 1988.
- Hindman, B. W. & Brown, T. M. *ApJ*, 504, 1029, 1998.
- Howe, R., Komm, R., & Hill, F. *ApJ*, 524, 1084, 1999.
- Jiménez-Reyes, S. J., Corbard, T., Pallé, P. L., Roca Cortés, T., & Tomczyk, S. *A&A*, 379, 622, 2001.
- Jiménez-Reyes, S.J., 2000, Ph.D. thesis, Univ. La Laguna, Tenerife, (2000)
- Kuhn, J. in *Helio- and Astero-seismology at the Dawn of the millennium (ESA SP-464)*, p. 7, 2000.
- Kuhn, J. *ApJ*, 331, L131, 1988.
- Kuhn, J. R. & Stein, R. F. 1996, *ApJ*, 463, L117
- Leibacher, J. *et al. Science*, 272, 1282, 1996.
- Libbrecht, K. Woodard, M.F. *Nature*, 345, 779, 1990.
- Moreno-Insertis, F. Schüssler, M., Ferris-Mas, A. *A&A*, 264, 686, 1992.
- Paternó, L. in *Osaki and Shibahashi eds., Progress of Seismology of the Sun and Stars*, p. 41, 1990.
- Rajaguru, S. P., Basu, S., & Antia, H. M. *ApJ*, 563, 410, 2001.
- Schou, J. *ApJ*, 523, L181, 1999.
- Thompson, M.J., 1995, *Inverse Problems*, 11, 709
- Tomczyk, P., Schou, J., Thompson M.J., 1995, *ApJ*, 448, L57
- Vorontsov, S. in *Helio- and Astero-seismology at the Dawn of the millennium (ESA SP-464)*, p. 563, 2000.

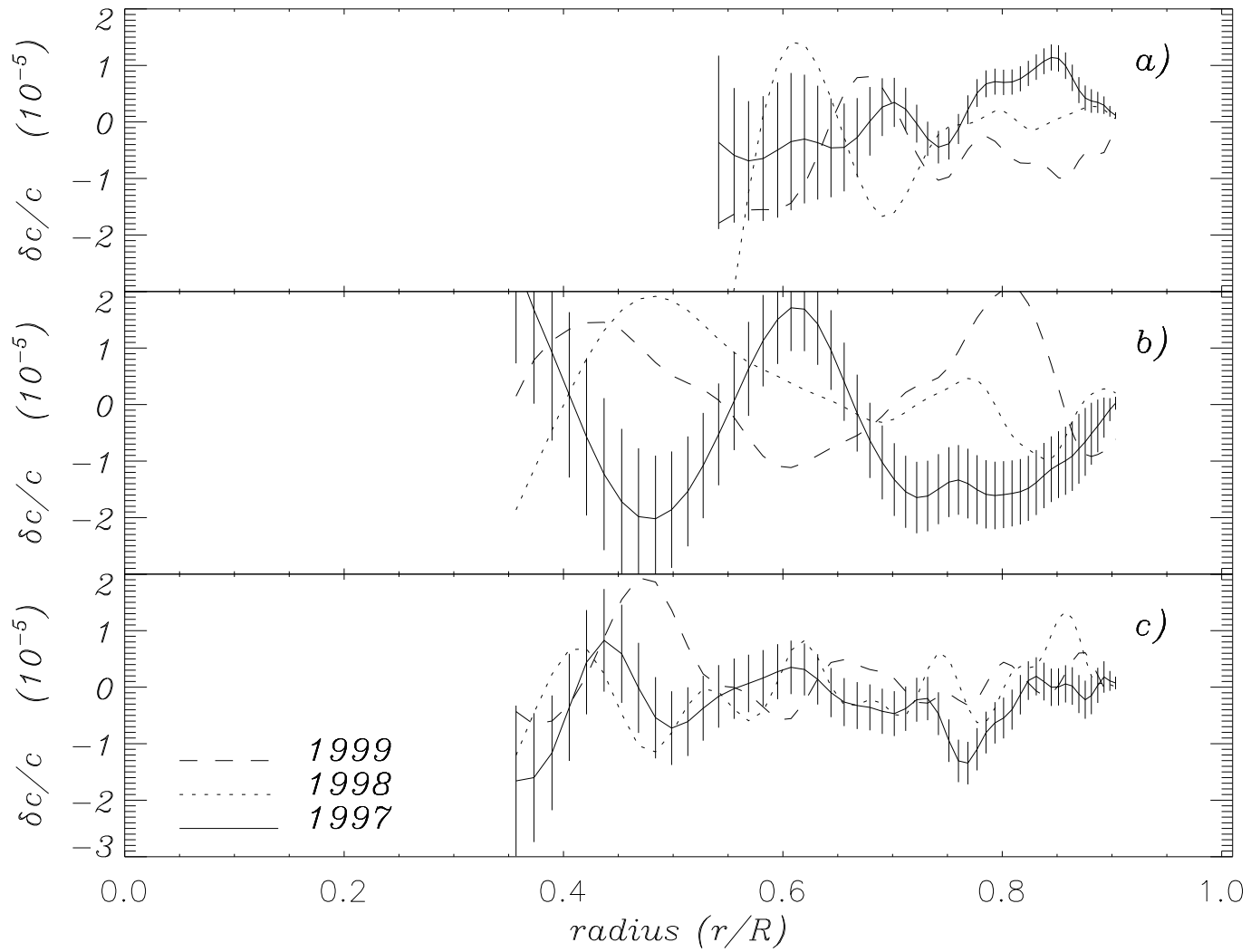


Fig. 1.— Relative sound speed differences inferred using 1-year-long averaged GONG (panel a), LOWL (panel b) and MDI (panel c) data, shown for clarity only for the years 1997, 1998 and 1999. The solutions are shown only where the inversions are reliable. For clarity, the error bars are only shown for the inversion of the 1997 data; the error bars of the other results are almost identical.

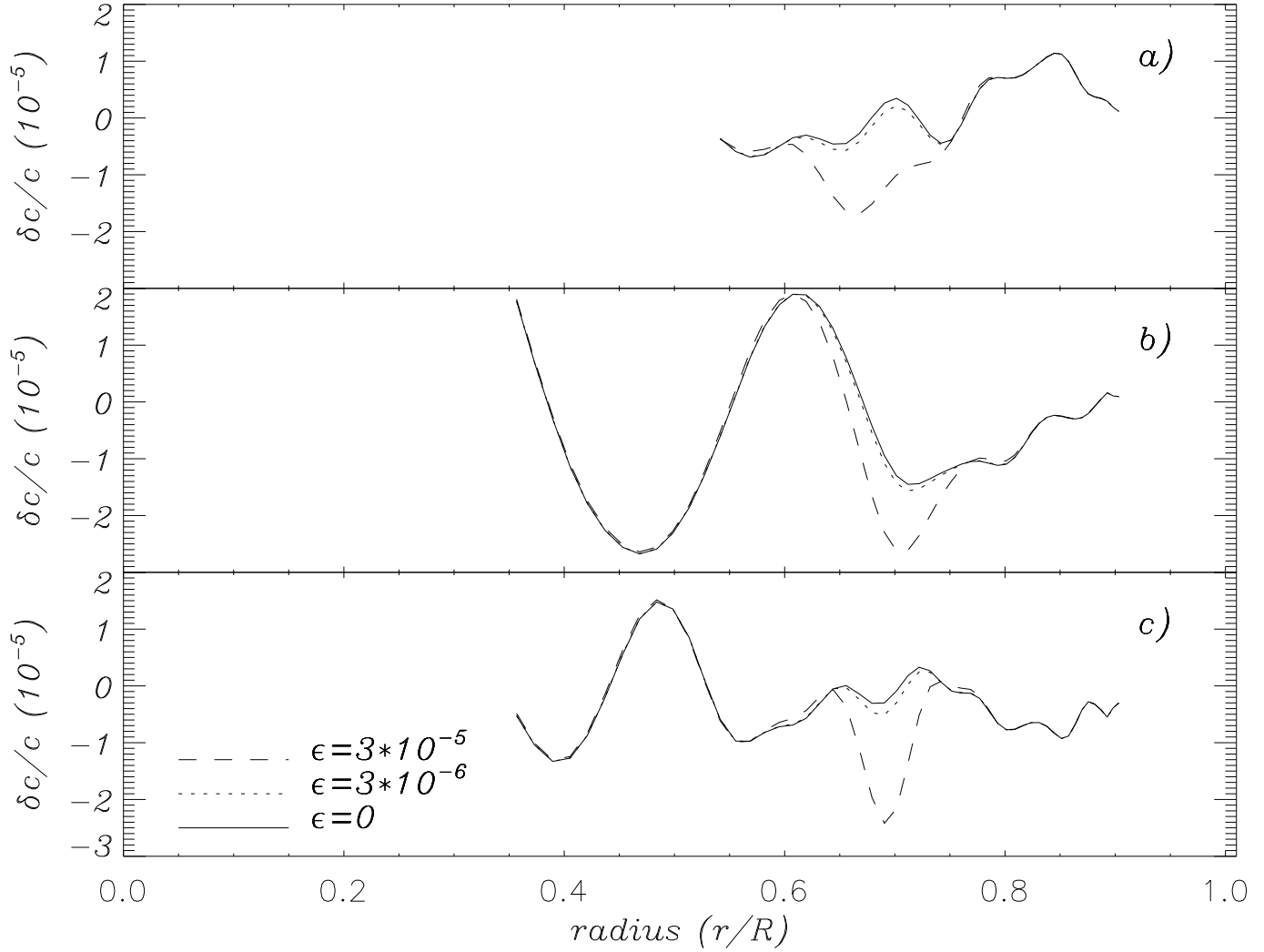


Fig. 2.— Relative sound speed differences inferred from the 1996 averaged GONG (panel a), LOWL (panel b) and MDI (panel c) data sets. For each panel, the solid line shows the inversion similar to those presented in Fig. 1, whereas the other two profiles correspond to inverted profiles from the same mode set but after the injection of a frequency change corresponding to a small perturbation in the sound speed between 0.68 and $0.70 R_{\odot}$, of amplitude $\epsilon = 3 \times 10^{-6}$ and 3×10^{-5} respectively. For clarity, error bars have not been included, although they are very similar to those shown in Figure 1.

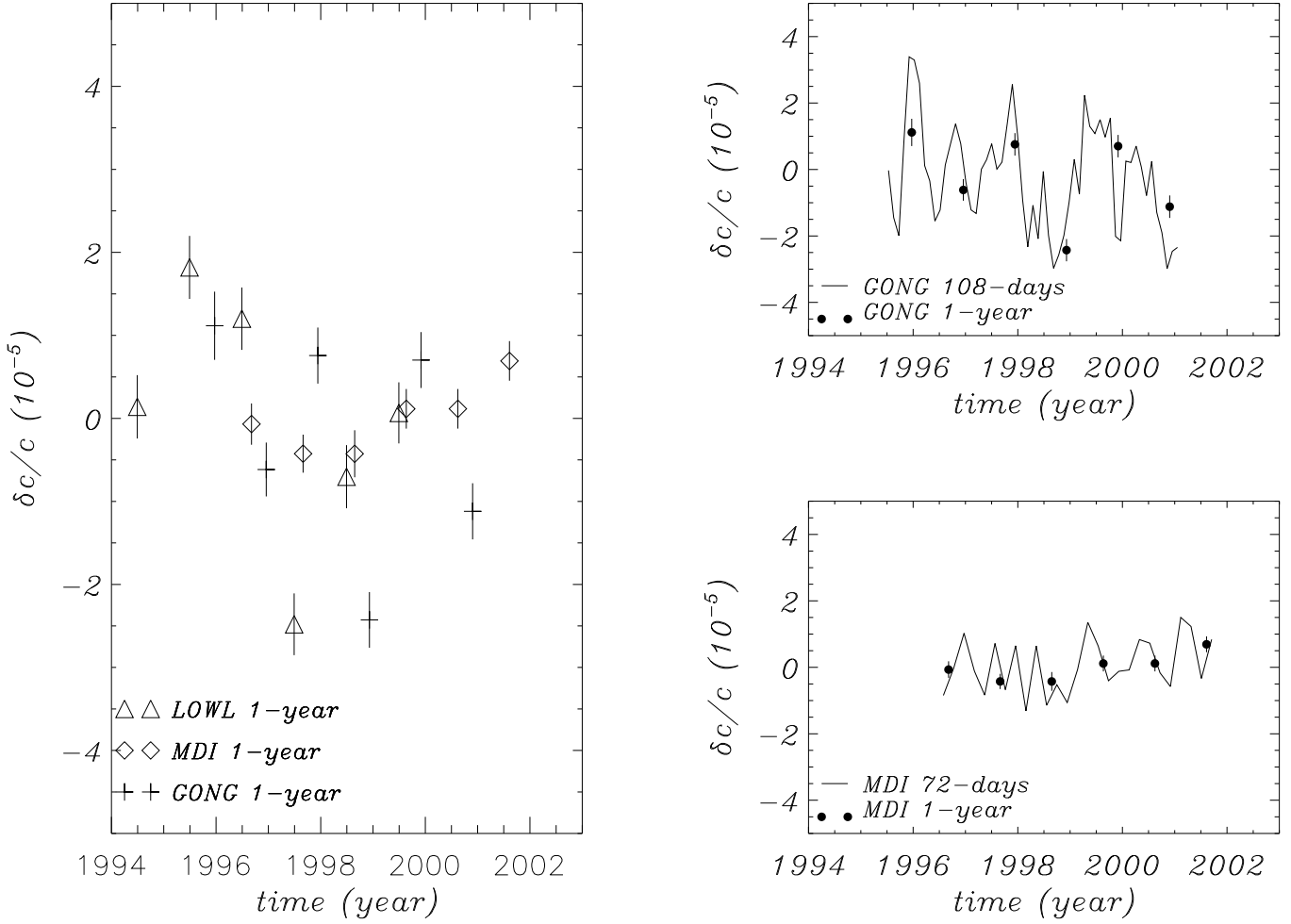


Fig. 3.— Temporal variations of the average of $\delta c/c$ at $r_0 = 0.69 R_\odot$ computed over the radial points that lie within the interval $0.69 \leq r/R_\odot \leq 0.72$. Left panel shows the results for LOWL, MDI and GONG 1-year-long data sets. Right panels compare results for the 108-day-long and 1-year-long GONG sets and the 72-day-long and 1-year-long MDI sets.

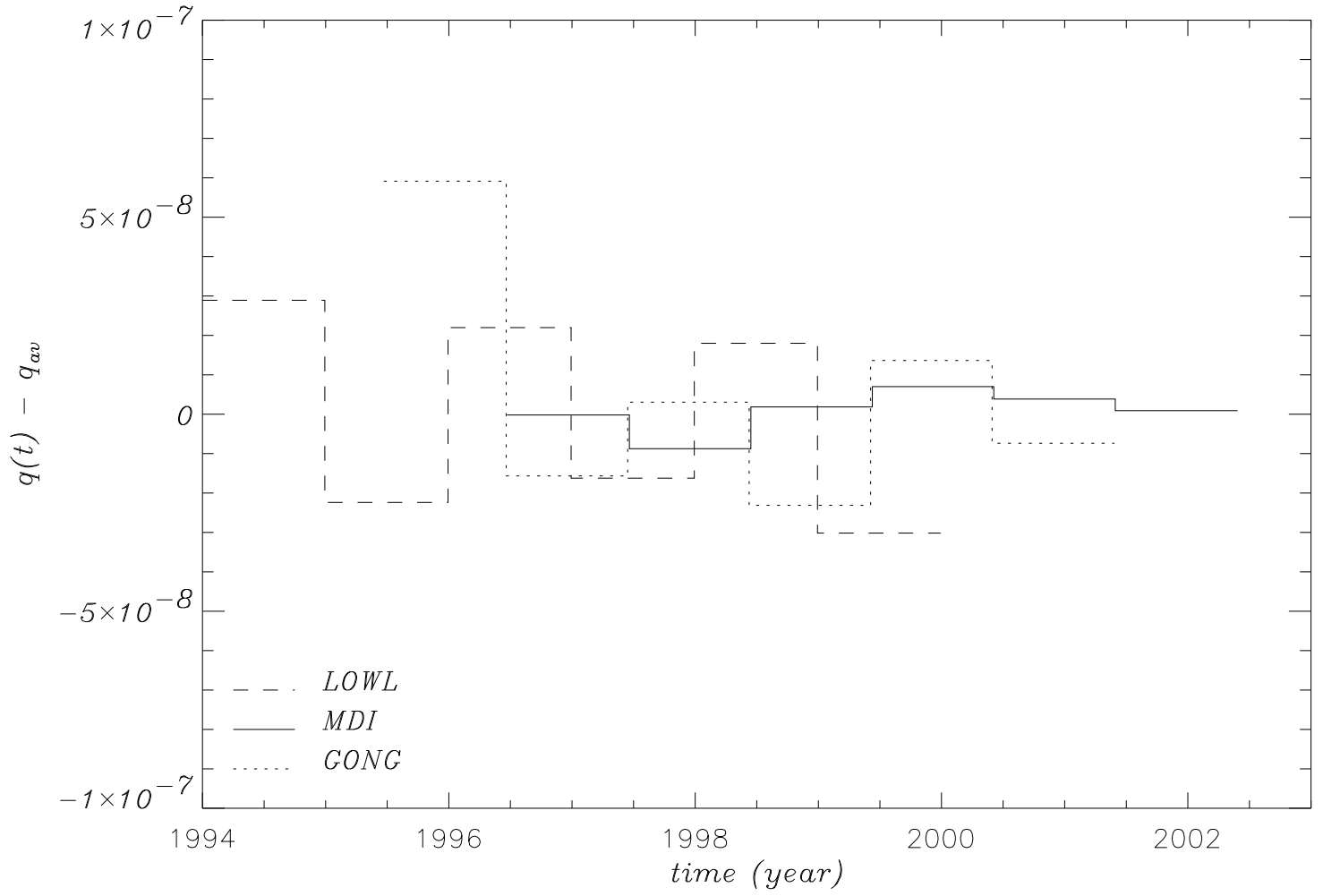


Fig. 4.— Contribution of the time-varying averaging kernel to spurious sound speed profile changes with time; see text for details.

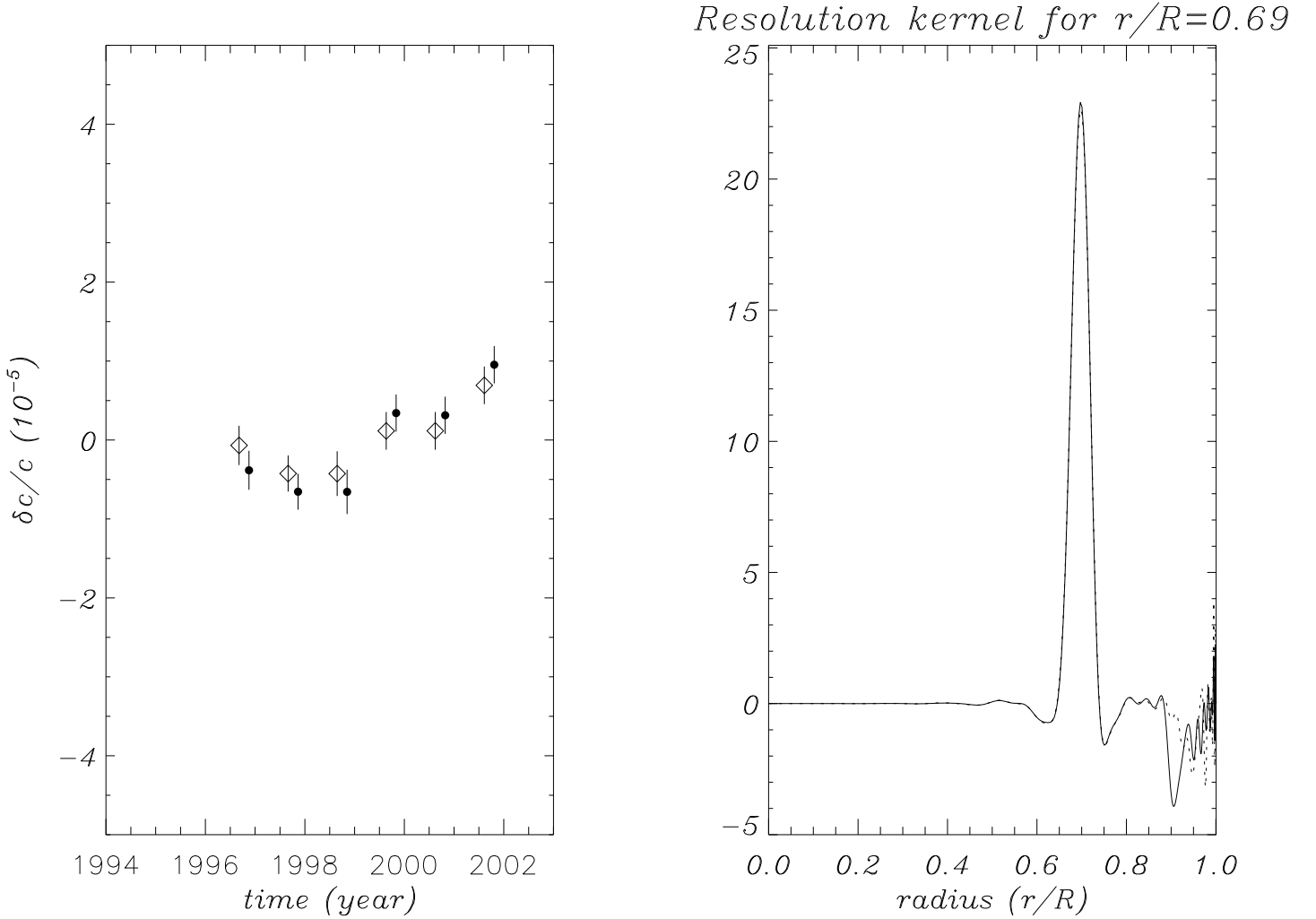


Fig. 5.— Left panel: temporal variations of the average of $\delta c/c$ over the radial points that lie within the interval $0.69 \leq r/R_{\odot} \leq 0.72$. Results correspond to 1-year-long MDI data with degrees expanding up to $l = 100$ (shown as diamonds) and $l = 150$ (shown as filled circles). Right panel: averaging kernels corresponding to the inversion of the 1996 data at $r = 0.69 R_{\odot}$. The solid line corresponds to the averaging kernel obtained from the inversion of data with degrees up to $l = 100$, while the dotted lines represents the averaging kernel obtained from the inversion of data with degrees up to $l = 150$.